HHS Public Access

Author manuscript

Exp Eye Res. Author manuscript; available in PMC 2016 July 01.

Published in final edited form as:

Exp Eye Res. 2015 July ; 136: 38–44. doi:10.1016/j.exer.2015.04.014.

Elevated intracranial pressure causes optic nerve and retinal ganglion cell degeneration in mice

Derek M. Nusbaum[a,b,c], **Samuel M. Wu**[c,d], and **Benjamin J. Frankfort**[b,d,*]

[a]Department of Internal Medicine, Baylor College of Medicine, Houston, TX

[b]Center for Space Medicine, Baylor College of Medicine, Houston, TX

[c]Department of Neuroscience, Baylor College of Medicine, Houston, Texas

[d]Department of Ophthalmology, Baylor College of Medicine, Houston, TX

Abstract

The purpose of this study was to develop a novel experimental system for the modulation and measurement of intracranial pressure (ICP), and to use this system to assess the impact of elevated ICP on the optic nerve and retinal ganglion cells (RGCs) in CD1 mice. This system involved surgical implantation of an infusion cannula and a radiowave based pressure monitoring probe through the skull and into the subarachnoid space. The infusion cannula was used to increase ICP, which was measured by the probe and transmitted to a nearby receiver. The system provided robust and consistent ICP waveforms, was well tolerated, and was stable over time. ICP was elevated to approximately 30 mmHg for one week, after which we assessed changes in optic nerve structure with transmission electron microscopy in cross section and RGC numbers with antibody staining in retinal flat mounts. ICP elevation resulted in optic nerve axonal loss and disorganization, as well as RGC soma loss. We conclude that the controlled manipulation of ICP in active, awake mice is possible, despite their small size. Furthermore, ICP elevation results in visual system phenotypes of optic nerve and RGC degeneration, suggesting that this model can be used to study the impact of ICP on the visual system. Potentially, this model can also be used to study the relationship between ICP and IOP, as well diseases impacted by ICP variation such as glaucoma, idiopathic intracranial hypertension, and the spaceflight-related visual impairment intracranial pressure syndrome.

[*]Author for correspondence: Baylor College of Medicine, Department of Ophthalmology, 6565 Fannin, NC – 205, Houston, TX, 77030, 713-798-3453, benjamin.frankfort@bcm.edu.

Conflict of interest statement:
The authors have no financial interest related to this work.

Keywords

retina; retinal ganglion cell; optic nerve; intracranial pressure; intraocular pressure: glaucoma; visual impairment intracranial pressure syndrome (VIIP syndrome); idiopathic intracranial hypertension (IIH)

1. Introduction

The optic nerve is made of retinal ganglion cell (RGC) axons and is located within the subarachnoid space (SAS). The RGC axons are exposed to constant pressure from two sources: intraocular pressure (IOP), which is transmitted within the eye posteriorly to the optic nerve head, and intracranial pressure (ICP), which is transmitted to the optic nerve at multiple points, including anteriorly to the optic nerve head. When either of these two pressures is increased in humans, deleterious consequences occur. Increased IOP may cause glaucoma, a neurodegenerative disease of the optic nerve and RGCs which is common among the elderly and is the second leading cause of blindness in the world (Gordon et al., 2002; Quigley and Broman, 2006). Increased ICP may result in a variety of conditions according to the magnitude of the elevation. At severe elevations, papilledema occurs and visual loss can be rapid and significant. At less extreme elevations, diseases such as idiopathic intracranial hypertension (IIH) and the spaceflight-related visual impairment intracranial pressure (VIIP) syndrome induce moderate, chronic visual changes (Acheson, 2006; Mader et al., 2011; Wall et al., 2014). In IIH, many patients also show evidence of optic nerve axon loss and RGC death (Keltner et al., 2014; Marzoli et al., 2013; Monteiro and Afonso, 2014; Padhye et al., 2013). Several reports have suggested that the balance between IOP and ICP is an important factor in optic neuropathies in general (Berdahl et al., 2008a; Berdahl et al., 2008b; Fleischman and Berdahl, 2014; Ren et al., 2010; Ren et al., 2011; Zhang and Hargens, 2014).

The anatomic effect of elevated IOP on the mouse visual system has been well-studied (Chen et al., 2011; Cone et al., 2010; Frankfort et al., 2013; Gross et al., 2003; Grozdanic et al., 2003; Ji et al., 2005; McKinnon et al., 2009; Ruiz-Ederra and Verkman, 2006; Samsel et al., 2011; Sappington et al., 2010). However, direct testing of the effects of elevated ICP on the visual system in mice has not been possible due to the lack of a suitable model for both the sustained elevation and accurate measurement of ICP. Thus, our current understanding of the effects of ICP in mice is limited to sedated animals in which ICP was elevated only for short periods of time, and we currently have no established system with which to potentially study the interaction between ICP and IOP in mice (Feiler et al., 2010; Ren et al., 2013). Fortunately, models of ICP monitoring have been developed in rodents as well as primates, so some of these critical relationships are experimentally accessible (Barth et al., 1992; Kusaka et al., 2004; Lin and Liu, 2010; Chowdhury et al., 2013; Silasi et al., 2009; Yang et al., 2014). However, the expansion of this approach into a genetically tractable organism such as mice would be beneficial.

We therefore developed a novel experimental system to modulate ICP in living, awake mice for an extended period of time. This system includes dual implantation of an infusion cannula and a radiowave based pressure monitoring probe through the skull and into the

SAS. The infusion cannula is then used to increase ICP, which is measured directly by the nearby probe and transmitted to a receiver in real time. We validated this system and then used it to chronically increase ICP in wild type CD1 mice and study its effects on optic nerve structure and RGC number. We found that ICP elevation results in marked optic nerve axonal loss and disorganization, as well as prominent RGC loss. This system indicates that controlled manipulation of ICP levels is possible in mice. This method can be used to study the effects of ICP change and potentially the ICP – IOP relationship in a variety of ophthalmologic and neurologic conditions.

2. Methods

2.1. Animals

All protocols and procedures were approved by the Baylor College of Medicine Animal Care and Use Committee and comply with federal guidelines and the ARVO statement for animal research. Eight-week-old, female, CD1 mice were maintained according to a standard 12 hour light – dark cycle.

2.2. Generation of ICP monitoring and modulation system

Animals were anesthetized with a weight-based intraperitoneal injection of ketamine (80mg/kg), xylazine (16mg/kg), and acepromazine (1.2mg/kg). Subsequently, the hair on the scalp was shaved with a standard pair of clippers. A 1cm midline incision starting at the base of the skull and directed anteriorly was fashioned using a #11 scalpel blade to expose the bony surface of the skull. A 1mm hole was drilled 1mm lateral and 1mm posterior to bregma on the right side of the animal. The dura was nicked with a 30 gauge needle to ensure an egress of cerebrospinal fluid (CSF) and entrance into the SAS. A custom cannula made from a 1.57mm diameter x 2.4mm long nylon screw (Plastics One, Inc.) with a hole drilled through the center lengthwise using a 0.4mm drill bit was positioned in the 1mm hole and anchored into the skull using 3M ESPE Durelon Carboxylate Luting Cement (3M). The cannula was slightly oversized to facilitate a tight seal. The tip of a PA-C10 pressure-monitoring probe (Data Sciences International) was fed through the hole in the center of the cannula into the SAS to allow for measurement of ICP. The inner diameter of the cannula was chosen to allow for a tight seal with the PA-C10 pressure-monitoring probe. A second 1mm hole was drilled 1mm lateral and 1mm posterior to bregma on the left side of the animal and the dura nicked as above. Prior to the surgery, a custom infusion cannula was made by placing a 23G syringe needle through a nylon screw, removing the hub, heat sealing it in place, and filing off the bevel was fashioned. This cannula was then positioned in the second 1mm hole and anchored into the skull as above. The entire system was held in place with a mound of silicone caulk which included both cannulas and the anterior-most segment of the PA-C10 monitoring probe (Figure 1). Subsequently, a 0.6cm transverse incision was made 2-3mm posterior to the base of the skull and a pocket made by blunt dissection subcutaneously over the back. The pressure probe transmitter was placed in this pocket between and past the scapulae of the animals and onto the mid-back, where it was sutured in place with 6.0 vicryl, interrupted sutures.

To evaluate the telemetry pressure monitoring system for stability, a cohort of animals (n = 6) was monitored for 3 weeks. These mice had their infusion cannula sealed off to ambient air by attaching a small length of PE50 tubing to the cannula and heat-sealing it with a soldering iron. ICP measurements were then recorded for 1 hour at 1 day, 1 week, 2 weeks, and 3 weeks post-operatively. For ICP elevation experiments, 6 animals were exposed to elevated ICP and 6 animals received cannula placement without ICP elevation. In the ICP elevation group, the infusion cannulas were attached to a fluid bag filled with artificial CSF (124mM NaCl, 2.5mM KCl, 2.0mM $MgSO_4$, 1.25mM KH_2PO_4, 26mM $NaHCO_3$, 10mM glucose, 4mM sucrose, 2.5mM $CaCl_2$) via PE50 tubing. The fluid bag was hung to gravity to empirically raise ICP to 30mmHg and remained at the same point for the duration of the study. In the control group, the infusion cannula was sealed off as for the stability experiments. In both groups, ICP was monitored for one hour each day for seven consecutive days. For all animals, sessions of ICP recording lasted one hour, and the mean value of each one hour block of time was calculated to get an average of ICP for that time point. ICP data for experiments were collected wirelessly by the PhysioTel® Small Animal Telemetry system and receivers and outputted to an excel spreadsheet using Ponemah Software 5.20 data analysis software (all from Data Sciences International; St. Paul, MN). This software automatically uploads raw data into a Microsoft Office Excel file for analysis.

2.3 Measurement of IOP

IOP was recorded using a rebound tonometer optimized for mouse use (Tonolab) under isoflurane anesthesia as previously described (Frankfort et al., 2013; Khan et al., 2015; Pease et al., 2011).

2.4. Preparation of optic nerves and retinas

Eyes and optic nerves were dissected out according to established protocols (Frankfort et al., 2013; Gross et al., 2003; Pang and Wu, 2011). Optic nerves were severed from the globe and fixed in 3% glutaraldehyde for up to 72 hours. Nerves were then washed with 0.1M sodium phosphate (pH = 7.3), post-fixed in 1% phosphate-buffered osmium tetroxide for 2 hours and dehydrated in a series of graded ethanol washes. Nerves were then infiltrated with acetone and embedded in plastic molds with 100% plastic resin (PolyBed 812, Polysciences, Inc.; Warrington, PA). Nerves were oriented so that a cross section of the optic nerve could be visualized. A Leica Ultracut R ultramicrotome fit with a diamond knife was used to cut 1 micron sections which were stained with 1% Toluidine Blue for 30 seconds to confirm orientation and quality of preparation. Additional 80–90 nanometer ultra-thin sections were then cut and enhanced with uranyl acetate followed by lead citrate for 10 minutes each. Images of the ultra-thin sections were then taken using a Zeiss EM902 transmission electron microscope (Carl Zeiss). Eight random regions equidistant between the center of the nerve and the periphery as well as two regions in the center of the nerve were imaged at 3000X magnification and captured with an AMT V602 digital camera. The identity of these regions was masked and myelinated axons counted manually for all ten regions by a single investigator with assistance from ImageJ software. This generated the axon density, which was converted to total axons (axons per optic nerve) by multiplying by the cross sectional optic nerve area (Levkovitch-Verbin et al., 2002; Mabuchi et al., 2003). The area of each

counted region was approximately 625 μm^2, such that the ten regions together represented about 5–6% of the total optic nerve cross sectional area.

RGCs in retinal flat mounts were stained with primary antibody to beta-III-tubulin (TUJI, 1:200, mouse; Covance, Emeryville, CA) and visualized with Alexa Fluor® 488 donkey anti-mouse secondary antibody (1:300; Life Technologies, Grand Island, NY). Images for RGC counting were acquired with a laser confocal microscope at 40x magnification (LSM 510; Carl Zeiss) and processed with Zeiss LSM-PC software (Carl Zeiss) and Adobe Photoshop CS5 (Adobe, Inc.). Four regions equidistant between the optic nerve and the peripheral retina as well as four additional regions equidistant between the first four regions and the peripheral retina were imaged from each eye as previously described (Frankfort et al., 2013). The identity of these regions was masked and tubulin-positive cells counted manually from all eight regions by a single investigator, assisted by ImageJ software. Cell counts were then converted into RGC density (RGCs/mm^2).

2.5. Statistical analysis

To determine if the pressure recordings were stable with time, a one-way analysis of variance was performed. To evaluate for a difference in ICP between control and elevated ICP groups, a two-way analysis of variance was performed. Students paired t-tests were used to evaluate the difference in RGC and optic nerve fiber counts for elevated ICP versus control groups. All statistical analysis was performed using Prism Software (GraphPad) or SPSS, Version 22 (IBM) with a cutoff of $p < 0.05$ as statistically significant.

3. Results

3.1. Development and verification of ICP modulation and measurement system

Animal surgery was performed and data collected as described in the Methods. During each surgery we first sought to ensure that our system was correctly positioned in the SAS and accurately measuring ICP. First, we confirmed that both cannulas were communicating directly with the SAS and were collocated in a contiguous fluid compartment. This was done during the surgery, after both cannulas were positioned but before the probe was placed, and was achieved by injecting artificial CSF through one cannula and watching for immediate egress through the other cannula. Second, after the probe was placed, we confirmed that we were truly measuring ICP by sampling our data-monitoring stream at high frequency to demonstrate a high fidelity ICP waveform with signature respiratory and pulse pressure variations (Figure 2A). Measured levels of ICP were in the expected physiologic range. Finally, we had additional confirmation once the surgery was complete because introduction of fluid to the SAS via artificial CSF injections caused an immediate rise in measured ICP. Taken together, these data confirmed that we were accurately measuring ICP in real time.

After mice recovered from surgery and anesthesia, they were not distressed from the procedure or from the implanted telemetry probe and the hardware did not appear to interfere with normal behaviors (Supplemental Video). There was a small degree of fluctuation in the ICP signal with movement around the cage in awake mice (Figure 2B). However, these fluctuations were minimal when the animals were at rest or asleep, and

respiratory and pulse pressure oscillations were still observable in the data stream (not shown).

To assess our system for suitability for long-term monitoring and to evaluate the signal for disruption and stability, we measured ICP weekly in six animals for a period of three weeks. ICP did not change over this time period ($p = 0.56$; Figure 2C). This suggests that the signal from the pressure monitoring system remains robust over time with stable ICP readings and without displacement of the hardware from normal animal activity.

Next, we determined that ICP could be elevated with our system. First, we acutely elevated ICP in an anesthetized mouse by raising the height of the artificial CSF infusion system to increase flow due to gravity. ICP increased rapidly and had no acute effect on IOP (Figure 3A). Note the “noise” in the ICP tracing after the elevation to 30 mmHg due to small fluctuations detected because of the high acquisition frequency (250 Hz) used in this experiment. We next elevated ICP to approximately 30 mmHg in a cohort of six mice and measured ICP daily for a period of one week. In two mice, IOP was also measured at daily time points under brief isoflurane anesthesia and IOP remained at baseline levels throughout (not shown). ICP remained stable across the one week study in both the control and elevated ICP group ($p = 0.89$). ICP was higher in the experimental group than in the control group ($p < 0.001$; Figure 3B).

3.2. Effect of ICP elevation on the visual system

We next sought to determine the impact of ICP elevation on optic nerve and RGC anatomy. At the end of the one week experiment, optic nerves and retinas were recovered from experimental animals and controls and processed for transmission electron microscopy and immunohistochemistry (Methods). Cross sectional images showed obvious disorganization of variable severity, and included dysmorphic and swollen appearing axons with vacuoles (Figure 4A–C). In many instances there was also decreased axonal staining, suggesting demyelination. Optic nerve axons were decreased in the elevated ICP group compared with the control group. The average axon count was 58,043 ± 5,048 in the control group, consistent with published norms (Fu and Sretavan, 2010; Mabuchi et al., 2003). The average axon count was 39,561 ± 1,941 in the elevated ICP group, representing a difference of 18,482 axons or a 31.8% decrease ($p = 0.014$; Figure 4D). No obvious nerve sheath dilation was detected at this position of the optic nerve.

We also assessed retinal ganglion cells (RGCs) in retinal flat mounts with an antibody to beta-III-tubulin, which has been shown to reliably label RGCs in several studies (Cui et al., 2003; Khan et al., 2014; Welsbie et al., 2013). We observed a marked reduction in RGC somas (Figure 5A, B). The average RGC count was 2,977 ± 75/mm^2 in the elevated ICP group and 3,713 ± 262/mm^2 in the control group for an average difference of 736 RGCs/mm^2 or 19.8% loss ($p = 0.022$; Figure 5C).

4. Discussion

4.1. A novel mouse model for ICP elevation

Clinical evidence suggests a potential relationship between ICP, IOP, and the visual system that may impact several neurological diseases including glaucoma, IIH, and the spaceflight-related VIIP syndrome. This relationship is thought to focus around pressure gradients across the optic nerve head, specifically the difference between ICP and IOP (Berdahl et al., 2008a; Berdahl et al., 2008b; Fleischman et al., 2012; Mader et al., 2011; Ren et al., 2010; Ren et al., 2011; Zhang and Hargens, 2014). Recent evidence from monkeys supports this relationship, and suggests that modeling in experimental animal systems is valuable (Yang et al., 2014). In this manuscript, we report a novel technique to modulate and measure ICP in living, awake mice. The ICP waveforms obtained are robust, and the technique provides accurate real-time measurements without noticeable pressure changes over a period of several weeks. The system also allows for rapid and accurate elevation of ICP both acutely and chronically, via infusion of artificial CSF into the SAS.

Multiple models for ICP measurement (Chavko et al., 2007; Kawoos et al., 2014; Lin and Liu, 2010; Silasi et al., 2009) or elevation (Bragin et al., 2013; Morrow et al., 1990; Park et al., 2011; Samuels et al., 2012; Xu et al., 2012) have been developed in rats. These studies have each been limited by a short duration of ICP elevation, a poorly predictable system for ICP elevation, brief ICP monitoring, a need for concurrent anesthesia, or some combination. Similar issues have impacted the few studies on ICP in mice as well (Feiler et al., 2010; Ren et al., 2013). To date, only one published report (in rats) has combined both ICP monitoring and modulation to specific levels, but no visual system phenotype was described (Chowdhury et al., 2013). Our model has several advantages over previously published attempts at chronic ICP modulation in rodents. First, by establishing this model in mice, the vast resources of mouse genetics are available for future mechanistic studies. Second, our model works well in active, awake mice. This flexibility potentially allows for the study of chronic ICP effects over a long period of time, as well as behavioral testing with mouse-optimized devices while exposed to altered ICP. Third, our model avoids damage to brain structures by cannulating the SAS instead of the lateral ventricle. While it is unlikely that surgery to position an infusion system in the lateral ventricle would cause direct damage to the visual pathways in the brain, the possibility of indirect events (hemorrhage, etc.) is nevertheless reduced. Fourth, our model uses a system in which the pressure sensor is closely linked in physical space to the SAS by a short tube within the probe. Previously published systems have often used a pressure sensor that is located in a region of the pressure monitoring system that is external to the animal. Thus, these systems may measure pressures inside the tubing system rather than pressure inside the skull. The two are assumed to be equivalent; however, with a small animal such as a mouse or rat, this assumption may not be appropriate. Several factors, including the large amount of dead space in the system relative to the size of the skull, high compliance of the system tubing, and the potential for leak, make these external pressure measurements potentially unreliable. The decreased opportunity for confounding factors in our system provides a higher likelihood of a precise ICP measurement.

4.2. Elevated ICP results in optic nerve and retinal ganglion cell degeneration

We used our new surgical system to chronically elevate ICP to a level of approximately 30mmHg for a period of one week. After this period of exposure, the optic nerve showed a prominent reduction in axons, as well as increased disorganization of the remaining axons and support structures including dysmorphic appearing cells and vacuoles (Figure 4). Cell counts of RGC somas were also similarly reduced, but to a lesser extent (Figure 5). This is therefore the first reported instance of visual system phenotypes associated with chronic ICP elevation in mice.

There are several possibilities for the observed phenotypes. One possibility is that elevated ICP results in global ICP-related effects on the brain and visual system including dilation of the optic nerve sheath with secondary axonal death, as is seen in multiple conditions associated with elevated ICP. Other possibilities, that the elevation in ICP results in ischemic or compressive effects on the optic nerve, are also plausible. A mass effect from a local infusion of artificial CSF could also occur. It is also possible that the site of axonal injury occurs far distally, even at the level of the lateral geniculate nucleus, which would also be exposed to conditions of elevated ICP. Lastly, secondary phenotypes related to altered ICP fluctuation due to forced elevation may occur. Additional anatomic, physiologic, and visual function experiments at more mild elevations of ICP (to reduce the potential impact of ischemia, compression, or mass effect) will help to distinguish among these possibilities and to determine the most direct human analog to this experimental model.

Interestingly, mouse models of experimental IOP elevation also show preferential loss of optic nerve tissue over RGCs and several groups have identified a time course of disease progression that begins with optic nerve injury and proceeds to RGCs (Buckingham et al., 2008; Chen et al., 2011; Cone et al., 2010; Crish et al., 2010; Sappington et al., 2010; Soto et al., 2008). It is therefore possible that increases in either ICP or IOP at the optic nerve head in mice result in a shared phenotype of optic nerve damage followed by RGC soma loss. This is potentially consistent with a biomechanical hypothesis of optic nerve damage in which the opposing forces of IOP and ICP interact to kink or bend the optic nerve fibers and surrounding structures (Fleischman and Berdahl, 2014). However, it is unlikely that an optic nerve head mechanism explains all the findings that have been observed with either elevated ICP or IOP. For example, much as experimental elevations of ICP are likely to impact the entire brain, including distal sites of the optic nerve axons and visual pathways, experimental elevations of IOP have also been shown to impact non-RGC retinal function in a number of reports (Frankfort et al., 2013; Holcombe et al., 2008; Pang et al., 2015). Future studies in which ICP and IOP are modulated simultaneously may be required to more fully probe this relationship in mice.

The impact of IOP elevation at the optic nerve head in mice is thought to also depend on a series of additional factors including age and genetic background (Cone et al., 2010; Cone et al., 2012). Our experiments were performed on young CD1 mice, a background that has been shown to be more susceptible to IOP-induced optic nerve injury than pigmented strains (Cone et al., 2010; Cone et al., 2012). Thus, a combination of ICP magnitude and genetic susceptibility may explain the rapidly occurring anatomic changes described in this

manuscript. Further study at lower ICP levels and in different genetic strains will therefore be helpful.

4.3. Interaction of ICP and IOP

In a limited number of animals, IOP was measured simultaneously with ICP and was shown to be unchanged in our model despite experimental manipulation of ICP (Figure 2). There is evidence for a common central regulation of ICP and IOP in rodents (Samuels et al., 2012). However, the mechanism by which changes in either ICP or IOP impacts the other is less clear, and there is conflicting clinical evidence regarding the causal relationship between ICP and IOP (Han et al., 2008; Sajjadi et al., 2006). Our data suggest that experimental elevation of ICP with our model does not impact IOP in mice, and that it may be possible to manipulate ICP and IOP independently. This approach would potentially allow for direct testing of ICP – IOP gradient effects on the optic nerve head, which could in turn validate or disprove clinical data regarding the ICP – IOP relationship. Such experiments could have significant implications for the treatment of several neurologic and ophthalmologic diseases.

5. Conclusions

We have developed a novel system for ICP measurement and modulation that allows for ICP elevation in active, awake mice. Using this system we found that one week of sustained ICP elevation resulted in both optic nerve and RGC phenotypes. These data suggest that experiments which chronically increase ICP in awake, non-sedated mice are possible, and provide a new opportunity to study the impact of ICP on the visual system. Potentially, this model can also be used to study the relationship between ICP and IOP, as well diseases impacted by ICP variation such as glaucoma, idiopathic intracranial hypertension, and the spaceflight-related visual impairment intracranial pressure syndrome.

Supplementary Material

Refer to Web version on PubMed Central for supplementary material.

Acknowledgments

Federal grant support for this project

NASA, NNX 10AK70G, Derek Nusbaum

NIH, EY019908, R01, Samuel Wu

NIH, EY002520, P30, Samuel Wu

NIH, EY021479, K08, Benjamin Frankfort

This work was supported by NASA Grant NNX 10AK70G (DMN), NIH Grants EY021479 (BJF), EY019908 (SMW), and EY02520 (Ophthalmology Core Grant to Baylor College of Medicine), the Retina Research Foundation (BJF and SMW), Research to Prevent Blindness (BJF and Baylor College of Medicine), and the Oshman Foundation (BJF). We thank Ralph Nichols for expert assistance with optic nerve preparations, staining, and imaging, and Guofu Shen for helpful discussion.

References

Acheson JF. Idiopathic intracranial hypertension and visual function. British medical bulletin. 2006; 79–80:233–244.

Barth KN, Onesti ST, Krauss WE, Solomon RA. A simple and reliable technique to monitor intracranial pressure in the rat: technical note. Neurosurgery. 1992; 30:138–140. [PubMed: 1738446]

Berdahl JP, Allingham RR, Johnson DH. Cerebrospinal fluid pressure is decreased in primary open-angle glaucoma. Ophthalmology. 2008a; 115:763–768. [PubMed: 18452762]

Berdahl JP, Fautsch MP, Stinnett SS, Allingham RR. Intracranial pressure in primary open angle glaucoma, normal tension glaucoma, and ocular hypertension: a case-control study. Invest Ophthalmol Vis Sci. 2008b; 49:5412–5418. [PubMed: 18719086]

Bragin DE, Bush RC, Nemoto EM. Effect of cerebral perfusion pressure on cerebral cortical microvascular shunting at high intracranial pressure in rats. Stroke. 2013; 44:177–181. [PubMed: 23204051]

Buckingham BP, Inman DM, Lambert W, Oglesby E, Calkins DJ, Steele MR, Vetter ML, Marsh-Armstrong N, Horner PJ. Progressive ganglion cell degeneration precedes neuronal loss in a mouse model of glaucoma. J Neurosci. 2008; 28:2735–2744. [PubMed: 18337403]

Chavko M, Koller WA, Prusaczyk WK, McCarron RM. Measurement of blast wave by a miniature fiber optic pressure transducer in the rat brain. J Neurosci Methods. 2007; 159:277–281. [PubMed: 16949675]

Chen H, Wei X, Cho KS, Chen G, Sappington R, Calkins DJ, Chen DF. Optic neuropathy due to microbead-induced elevated intraocular pressure in the mouse. Invest Ophthalmol Vis Sci. 2011; 52:36–44. [PubMed: 20702815]

Chowdhury UR, Holman BH, Fautsch MP. A novel rat model to study the role of intracranial pressure modulation on optic neuropathies. PLoS One. 2013; 8:e82151. [PubMed: 24367501]

Cone FE, Gelman SE, Son JL, Pease ME, Quigley HA. Differential susceptibility to experimental glaucoma among 3 mouse strains using bead and viscoelastic injection. Exp Eye Res. 2010; 91:415–424. [PubMed: 20599961]

Cone FE, Steinhart MR, Oglesby EN, Kalesnykas G, Pease ME, Quigley HA. The effects of anesthesia, mouse strain and age on intraocular pressure and an improved murine model of experimental glaucoma. Exp Eye Res. 2012; 99C:27–35. [PubMed: 22554836]

Crish SD, Sappington RM, Inman DM, Horner PJ, Calkins DJ. Distal axonopathy with structural persistence in glaucomatous neurodegeneration. Proc Natl Acad Sci U S A. 2010; 107:5196–5201. [PubMed: 20194762]

Cui Q, Yip HK, Zhao RC, So KF, Harvey AR. Intraocular elevation of cyclic AMP potentiates ciliary neurotrophic factor-induced regeneration of adult rat retinal ganglion cell axons. Mol Cell Neurosci. 2003; 22:49–61. [PubMed: 12595238]

Feiler S, Friedrich B, Scholler K, Thal SC, Plesnila N. Standardized induction of subarachnoid hemorrhage in mice by intracranial pressure monitoring. J Neurosci Methods. 2010; 190:164–170. [PubMed: 20457182]

Fleischman D, Berdahl JP. Posterior scleral biomechanics and the translaminar pressure difference. Int Ophthalmol Clin. 2014; 54:73–94. [PubMed: 24296373]

Fleischman D, Berdahl JP, Zaydlarova J, Stinnett S, Fautsch MP, Allingham RR. Cerebrospinal fluid pressure decreases with older age. PLoS One. 2012; 7:e52664. [PubMed: 23300737]

Frankfort BJ, Khan AK, Tse DY, Chung I, Pang JJ, Yang Z, Gross RL, Wu SM. Elevated intraocular pressure causes inner retinal dysfunction before cell loss in a mouse model of experimental glaucoma. Invest Ophthalmol Vis Sci. 2013; 54:762–770. [PubMed: 23221072]

Fu CT, Sretavan D. Laser-induced ocular hypertension in albino CD-1 mice. Invest Ophthalmol Vis Sci. 2010; 51:980–990. [PubMed: 19815738]

Gordon MO, Beiser JA, Brandt JD, Heuer DK, Higginbotham EJ, Johnson CA, Keltner JL, Miller JP, Parrish RK 2nd, Wilson MR, Kass MA. The Ocular Hypertension Treatment Study: baseline factors that predict the onset of primary open-angle glaucoma. Arch Ophthalmol. 2002; 120:714–720. discussion 829–730. [PubMed: 12049575]

Gross RL, Ji J, Chang P, Pennesi ME, Yang Z, Zhang J, Wu SM. A mouse model of elevated intraocular pressure: retina and optic nerve findings. Trans Am Ophthalmol Soc. 2003; 101:163–169. discussion 169–171. [PubMed: 14971574]

Grozdanic SD, Betts DM, Sakaguchi DS, Allbaugh RA, Kwon YH, Kardon RH. Laser-induced mouse model of chronic ocular hypertension. Invest Ophthalmol Vis Sci. 2003; 44:4337–4346. [PubMed: 14507878]

Han Y, McCulley TJ, Horton JC. No correlation between intraocular pressure and intracranial pressure. Ann Neurol. 2008; 64:221–224. [PubMed: 18570302]

Holcombe DJ, Lengefeld N, Gole GA, Barnett NL. Selective inner retinal dysfunction precedes ganglion cell loss in a mouse glaucoma model. Br J Ophthalmol. 2008; 92:683–688. [PubMed: 18296504]

Ji J, Chang P, Pennesi ME, Yang Z, Zhang J, Li D, Wu SM, Gross RL. Effects of elevated intraocular pressure on mouse retinal ganglion cells. Vision Res. 2005; 45:169–179. [PubMed: 15581918]

Kawoos U, Meng X, Huang SM, Rosen A, McCarron RM, Chavko M. Telemetric intracranial pressure monitoring in blast-induced traumatic brain injury. IEEE Trans Biomed Eng. 2014; 61:841–847. [PubMed: 24557686]

Keltner JL, Johnson CA, Cello KE, Wall M. Baseline visual field findings in the Idiopathic Intracranial Hypertension Treatment Trial (IIHTT). Invest Ophthalmol Vis Sci. 2014; 55:3200–3207. [PubMed: 24781936]

Khan AK, Tse DY, van der Heijden ME, Shah P, Nusbaum DM, Yang Z, Wu SM, Frankfort BJ. Prolonged elevation of intraocular pressure results in retinal ganglion cell loss and abnormal retinal function in mice. Exp Eye Res. 2015; 130:29–37. [PubMed: 25450059]

Kusaka G, Calvert JW, Smelley C, Nanda A, Zhang JH. New lumbar method for monitoring cerebrospinal fluid pressure in rats. J Neurosci Methods. 2004; 135:121–127. [PubMed: 15020096]

Levkovitch-Verbin H, Quigley HA, Martin KR, Valenta D, Baumrind LA, Pease ME. Translimbal laser photocoagulation to the trabecular meshwork as a model of glaucoma in rats. Invest Ophthalmol Vis Sci. 2002; 43:402–410. [PubMed: 11818384]

Lin JS, Liu JH. Circadian variations in intracranial pressure and translaminar pressure difference in Sprague-Dawley rats. Invest Ophthalmol Vis Sci. 2010; 51:5739–5743. [PubMed: 20574015]

Mabuchi F, Aihara M, Mackey MR, Lindsey JD, Weinreb RN. Optic nerve damage in experimental mouse ocular hypertension. Invest Ophthalmol Vis Sci. 2003; 44:4321–4330. [PubMed: 14507876]

Mader TH, Gibson CR, Pass AF, Kramer LA, Lee AG, Fogarty J, Tarver WJ, Dervay JP, Hamilton DR, Sargsyan A, Phillips JL, Tran D, Lipsky W, Choi J, Stern C, Kuyumjian R, Polk JD. Optic disc edema, globe flattening, choroidal folds, and hyperopic shifts observed in astronauts after long-duration space flight. Ophthalmology. 2011; 118:2058–2069. [PubMed: 21849212]

Marzoli SB, Ciasca P, Curone M, Cammarata G, Melzi L, Criscuoli A, Bussone G, D'Amico D. Quantitative analysis of optic nerve damage in idiopathic intracranial hypertension (IIH) at diagnosis. Neurol Sci. 2013; 34(Suppl 1):S143–145. [PubMed: 23695066]

McKinnon SJ, Schlamp CL, Nickells RW. Mouse models of retinal ganglion cell death and glaucoma. Exp Eye Res. 2009; 88:816–824. [PubMed: 19105954]

Monteiro ML, Afonso CL. Macular thickness measurements with frequency domain-OCT for quantification of axonal loss in chronic papilledema from pseudotumor cerebri syndrome. Eye (Lond). 2014; 28:390–398. [PubMed: 24406417]

Morrow BA, Starcevic VP, Keil LC, Seve WB. Intracranial hypertension after cerebroventricular infusions in conscious rats. Am J Physiol. 1990; 258:R1170–1176. [PubMed: 2337198]

Padhye LV, Van Stavern GP, Sharma A, Viets R, Huecker JB, Gordon MO. Association between visual parameters and neuroimaging features of idiopathic intracranial hypertension. J Neurol Sci. 2013; 332:80–85. [PubMed: 23850064]

Pang JJ, Frankfort BJ, Gross RL, Wu SM. Elevated intraocular pressure decreases response sensitivity of inner retinal neurons in experimental glaucoma mice. Proc Natl Acad Sci U S A. 2015; 112:2593–2598. [PubMed: 25675503]

Pang JJ, Wu SM. Morphology and immunoreactivity of retrogradely double-labeled ganglion cells in the mouse retina. Invest Ophthalmol Vis Sci. 2011; 52:4886–4896. [PubMed: 21482641]

Park YS, Park SW, Suk JS, Nam TK. Development of an acute obstructive hydrocephalus model in rats using N-butyl cyanoacrylate. Childs Nerv Syst. 2011; 27:903–910. [PubMed: 21286731]

Pease ME, Cone FE, Gelman S, Son JL, Quigley HA. Calibration of the TonoLab tonometer in mice with spontaneous or experimental glaucoma. Invest Ophthalmol Vis Sci. 2011; 52:858–864. [PubMed: 20720229]

Quigley HA, Broman AT. The number of people with glaucoma worldwide in 2010 and 2020. Br J Ophthalmol. 2006; 90:262–267. [PubMed: 16488940]

Ren R, Jonas JB, Tian G, Zhen Y, Ma K, Li S, Wang H, Li B, Zhang X, Wang N. Cerebrospinal fluid pressure in glaucoma: a prospective study. Ophthalmology. 2010; 117:259–266. [PubMed: 19969367]

Ren R, Wang N, Zhang X, Cui T, Jonas JB. Trans-lamina cribrosa pressure difference correlated with neuroretinal rim area in glaucoma. Graefes Arch Clin Exp Ophthalmol. 2011; 249:1057–1063. [PubMed: 21455776]

Ren Z, Iliff JJ, Yang L, Yang J, Chen X, Chen MJ, Giese RN, Wang B, Shi X, Nedergaard M. 'Hit & Run' model of closed-skull traumatic brain injury (TBI) reveals complex patterns of post-traumatic AQP4 dysregulation. J Cereb Blood Flow Metab. 2013; 33:834–845. [PubMed: 23443171]

Ruiz-Ederra J, Verkman AS. Mouse model of sustained elevation in intraocular pressure produced by episcleral vein occlusion. Exp Eye Res. 2006; 82:879–884. [PubMed: 16310189]

Sajjadi SA, Harirchian MH, Sheikhbahaei N, Mohebbi MR, Malekmadani MH, Saberi H. The relation between intracranial and intraocular pressures: study of 50 patients. Ann Neurol. 2006; 59:867–870. [PubMed: 16634008]

Samsel PA, Kisiswa L, Erichsen JT, Cross SD, Morgan JE. A novel method for the induction of experimental glaucoma using magnetic microspheres. Invest Ophthalmol Vis Sci. 2011; 52:1671–1675. [PubMed: 20926815]

Samuels BC, Hammes NM, Johnson PL, Shekhar A, McKinnon SJ, Allingham RR. Dorsomedial/Perifornical hypothalamic stimulation increases intraocular pressure, intracranial pressure, and the translaminar pressure gradient. Invest Ophthalmol Vis Sci. 2012; 53:7328–7335. [PubMed: 23033392]

Sappington RM, Carlson BJ, Crish SD, Calkins DJ. The microbead occlusion model: a paradigm for induced ocular hypertension in rats and mice. Invest Ophthalmol Vis Sci. 2010; 51:207–216. [PubMed: 19850836]

Silasi G, MacLellan CL, Colbourne F. Use of telemetry blood pressure transmitters to measure intracranial pressure (ICP) in freely moving rats. Curr Neurovasc Res. 2009; 6:62–69. [PubMed: 19355927]

Soto I, Oglesby E, Buckingham BP, Son JL, Roberson ED, Steele MR, Inman DM, Vetter ML, Horner PJ, Marsh-Armstrong N. Retinal ganglion cells downregulate gene expression and lose their axons within the optic nerve head in a mouse glaucoma model. J Neurosci. 2008; 28:548–561. [PubMed: 18184797]

Wall M, Kupersmith MJ, Kieburtz KD, Corbett JJ, Feldon SE, Friedman DI, Katz DM, Keltner JL, Schron EB, McDermott MP, Group NIIHS. The idiopathic intracranial hypertension treatment trial: clinical profile at baseline. JAMA neurology. 2014; 71:693–701. [PubMed: 24756302]

Welsbie DS, Yang Z, Ge Y, Mitchell KL, Zhou X, Martin SE, Berlinicke CA, Hackler L Jr, Fuller J, Fu J, Cao LH, Han B, Auld D, Xue T, Hirai S, Germain L, Simard-Bisson C, Blouin R, Nguyen JV, Davis CH, Enke RA, Boye SL, Merbs SL, Marsh-Armstrong N, Hauswirth WW, DiAntonio A, Nickells RW, Inglese J, Hanes J, Yau KW, Quigley HA, Zack DJ. Functional genomic screening identifies dual leucine zipper kinase as a key mediator of retinal ganglion cell death. Proc Natl Acad Sci U S A. 2013; 110:4045–4050. [PubMed: 23431148]

Xu H, Tan G, Zhang S, Zhu H, Liu F, Huang C, Zhang F, Wang Z. Minocycline reduces reactive gliosis in the rat model of hydrocephalus. BMC Neurosci. 2012; 13:148. [PubMed: 23217034]

Yang D, Fu J, Hou R, Liu K, Jonas JB, Wang H, Chen W, Li Z, Sang J, Zhang Z, Liu S, Cao Y, Xie X, Ren R, Lu Q, Weinreb RN, Wang N. Optic neuropathy induced by experimentally reduced

cerebrospinal fluid pressure in monkeys. Invest Ophthalmol Vis Sci. 2014; 55:3067–3073. [PubMed: 24736050]

Zhang LF, Hargens AR. Intraocular/Intracranial pressure mismatch hypothesis for visual impairment syndrome in space. Aviat Space Environ Med. 2014; 85:78–80. [PubMed: 24479265]

Highlights

- We developed a novel system with which to measure and modulate intracranial pressure in mice.
- We studied mice exposed to elevated intracranial pressure for one week.
- We examined changes in optic nerve appearance and retinal ganglion cell number.
- After intacranial pressure elevation, optic nerve axon and retinal ganglion cell soma loss were prominent

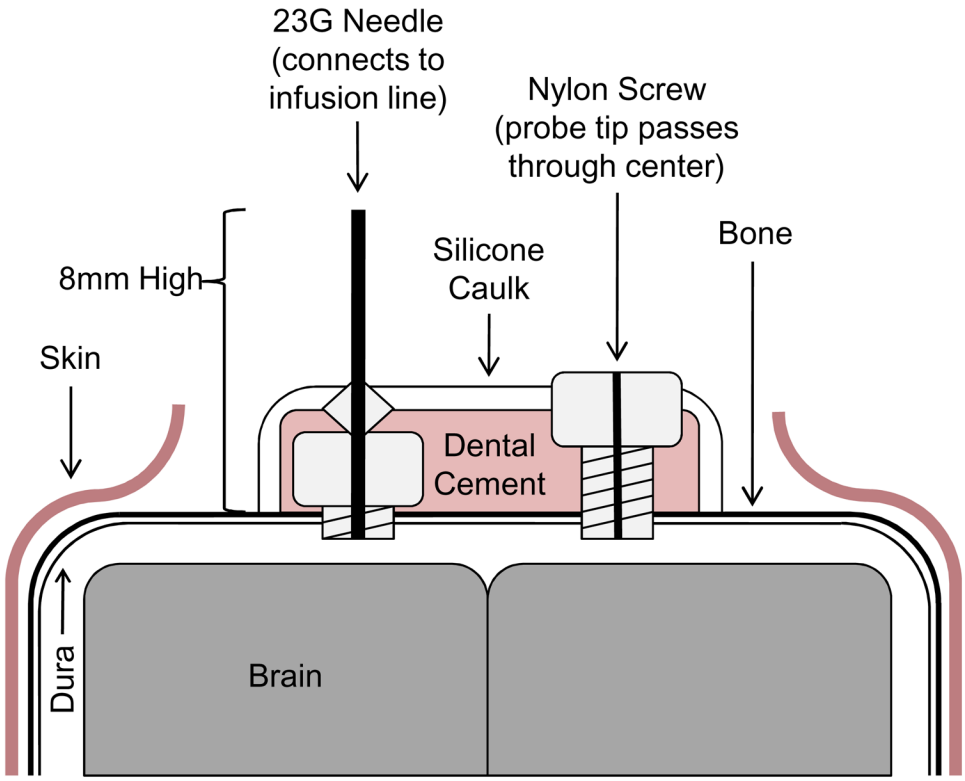

Figure 1. Schematic of surgical complex for ICP modulation and measurement

Animal surgery for the elevation and measurement of ICP is described in section 2.2 of the Methods. A coronal view of the final surgical complex is shown.

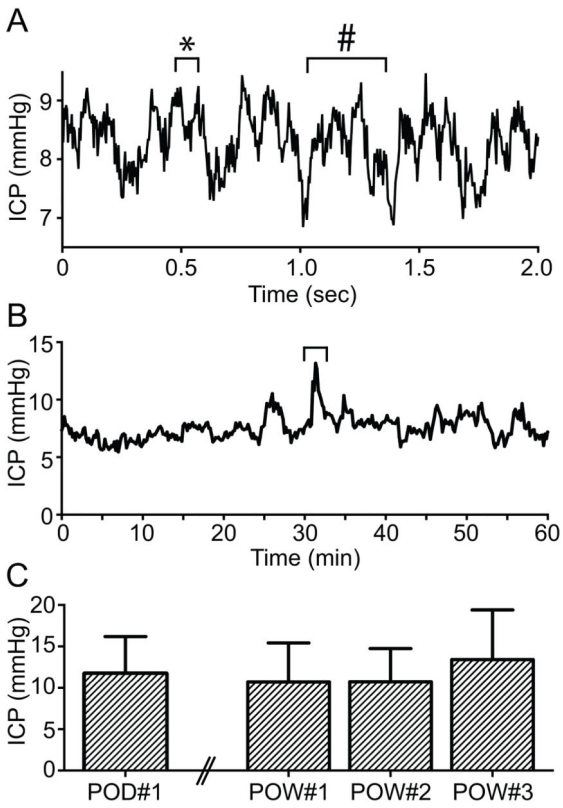

Figure 2. ICP waveform and stability

A. A two second window of ICP recording at 250 Hz data acquisition frequency. Note the pattern of respiratory (#) and pulse pressure (*) variations in the pressure recordings, consistent with accurate placement of the pressure catheter and recording of ICP. B. A one hour ICP monitoring session of an awake 8 week old CD1 mouse at 4 Hz data acquisition frequency. Note the slight variation in ICP with activity just after the 30 minute time point (bracket). C. Weekly ICP measurements in six mice for 3 weeks, demonstrating a stable ICP signal over time. ICP for each mouse at each time point was calculated as an average of 1 hour data collection at 4 Hz. Error bars represent one SEM. Note the difference in time scale along the X axis in panels A and B. Note the differences in scale of the Y axis among all panels.

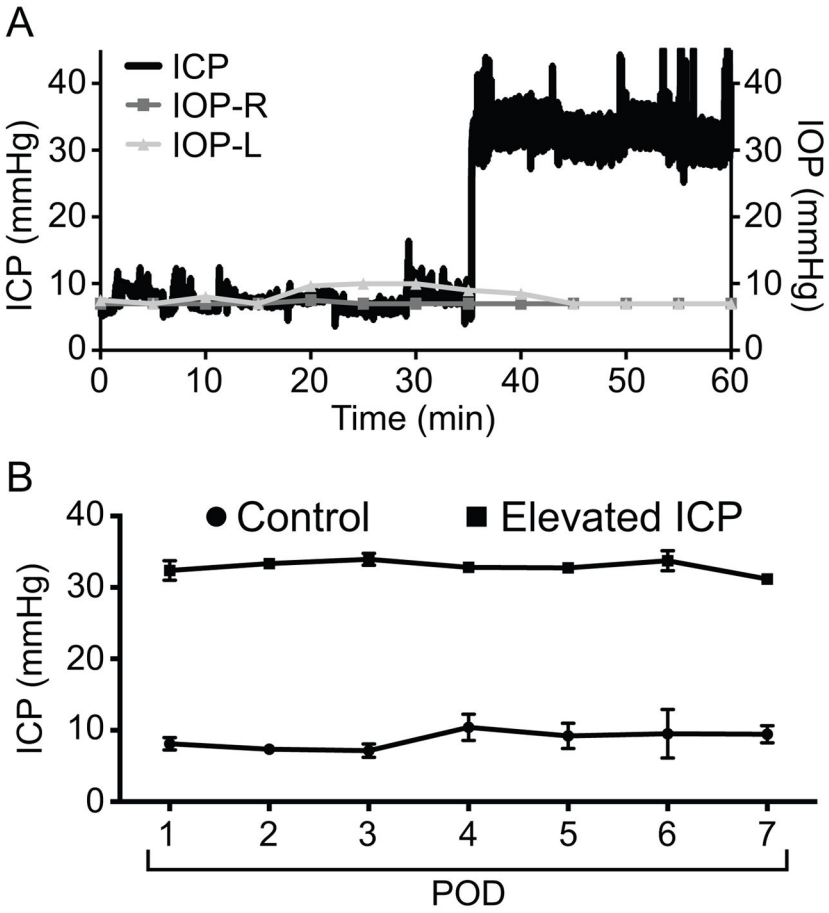

Figure 3. ICP elevation is stable and does not impact IOP

A. Acute ICP elevation in an anesthetized mouse. ICP rose to approximately 30 mmHg immediately after increasing artificial CSF flow. IOP was measured every 5 minutes before and after acute ICP elevation and did not change in either eye. ICP measurements in this panel were collected at 250 Hz. B. Daily post-operative (POD = post-operative day) ICP measurements in mice exposed to sustained elevated ICP (elevated ICP, squares; n = 6) or normal ICP (control, circles; n = 6). ICP was originally at baseline (as in panel A) prior to elevation of ICP. Once elevated, ICP was maintained at the same level for the duration of the study. ICP was significantly higher in the experimental group. At some time points the error bars (one SEM) were so small that they were beyond the resolution of the figure. ICP for each mouse at each time point was calculated as an average of 1 hour data collection at 4 Hz.

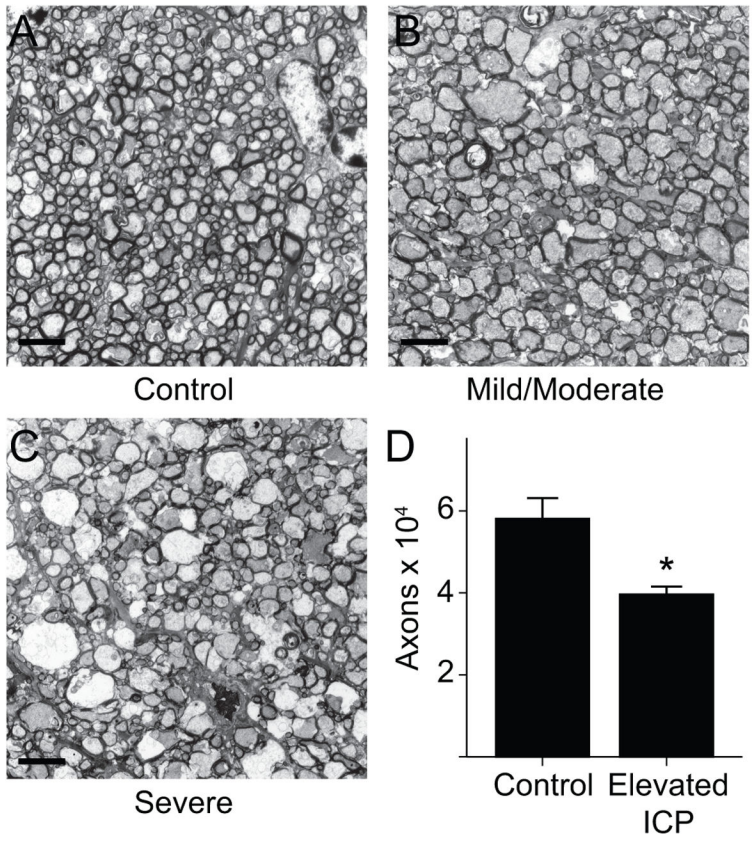

Figure 4. Optic nerve changes following chronic ICP elevation

A–C. 3000x images taken with an electron microscope of sectioned optic nerves at the same position located 2 mm posterior to the globe and enhanced with uranyl acetate and lead citrate (scale bar = 4 μm). A. Example of a control optic nerve. Axons are tightly packed with predominantly small diameters. B. Example of an optic nerve exposed to elevated ICP with mild to moderate changes. Some axons are larger in diameter and there is mild disorganization of the overall nerve structure including dysmorphic cells, swollen axons, and decreased axonal staining. C. Example of an optic nerve exposed to elevated ICP with severe changes. Many axons are larger in diameter and there is prominent disorganization of the overall nerve structure including gross axon swelling, many dysmorphic cells and further decreased axonal staining. D. Bar graph showing axons count per optic nerve. There are fewer optic nerve axons in the elevated ICP group (t-test, $p = 0.014$; $n = 4$ for each group). Error bars represent one SEM.

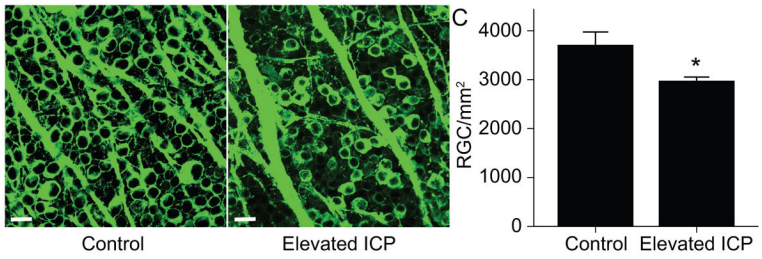

Figure 5. RGC changes following chronic ICP elevation

A–B. Images of retinal flat mounts from the same region of the retina labeled with antibody to beta-III tubulin taken with a confocal microscope at 40x magnification (scale bar = 20 μm). A. Example of a control retina. RGCs are confluent in flat mount preparation. B. Example of a retina exposed to elevated ICP. There are regions in which RGCs are absent. C. Bar graph showing RGC counts per mm^2 of flat mount retina. There are fewer RGCs in the elevated ICP group (t-test, $p = 0.022$; $n = 6$ for each group). Error bars represent one SEM.